Thermoelastic finite element model updating with application to monumental buildings

Thermo-elastic finite element model updating with application to monumental buildings

Rosario Ceravolo*, Giulia De Lucia, Gaetano Miraglia, Marica L. Pecorelli

DISEG (Politecnico di Torino), c. Duca degli Abruzzi 24, 10128 Torino, Italy

Abstract: A reliable and predictive model of an existing structure entails the use of model updating techniques, which are usually performed on the basis of operational modal analysis campaigns. In this paper, a new model calibration strategy is proposed that adopts a multiphysics approach to exploit data collected by both static and dynamic monitoring systems. More specifically, mechanical and temperature data are assimilated into the model through a thermo-elastic updating. The proposed scheme, complemented by a novel metaheuristic algorithm, is demonstrated in the case of the Sanctuary of Vicoforte, a complex historical building that is subjected to both static and dynamic monitoring.

1 INTRODUCTION

Finite Element Model (FEM) updating is a valuable tool in engineering applications to minimize the differences between test measurements and model prediction and therefore to obtain a more reliable numerical model (Mottershead & Friswell, 1993). The updated FEM can be employed for structural and dynamic analyses and can be used for Structural Health Monitoring (SHM). SHM is the process of developing and applying damage detection strategies in structures (Farrar and Worden, 2007).

Generally, model updating methods can be subdivided into two categories based on direct and iterative approaches. Both these methods are largely discussed in the literature (Sarmandi et al., 2016). In direct methods, which are commonly used for simple systems where a closed formulation is available, all the model parameters are updated in one step (Friswell et al., 2001). Instead, in iterative methods the use of optimisation algorithms is currently being explored to resolve the inverse problem of the calibration of the parameters.

It is worth mentioning that in the last years novel types of calibration have been proposed. For example, Artificial Neural Networks (ANN) (Siddique and Adeli, 2013; Villarrubia et al., 2018) can be used to create metamodels of the original FE model. Among many possible applications, these surrogate representations can emulate FE models in the calibration phase.

In order to distinguish among different types of updating, the term Modal Model Updating (MMU) is used when the global system mass and stiffness matrices are updated from experimentally identified modal quantities, typically limited to measured natural frequencies and shapes (Ramos et al., 2010), as modal damping data show higher dispersion (Ceravolo et al., 2017). However, in the more general case the FEM calibration process may consider parameters belonging to different physical fields (multiphysics updating), like in Thermo-Mechanical Model Updating (TMMU), where the thermal and mechanical parameters are updated in a holistic framework.

Despite the broad number of techniques implemented, direct methods are difficult to enforce, giving unsatisfactory results because of the quantity and the quality of experimental data required. Differently, iterative methods are generally based on FE modelling. FE models are a set of individual elements defined by their designed parameters, as geometry and/or material properties, so this approach introduces changes to a predefined number of parameters, in order to minimise a parameterised error.

The sequences required for solving the equations system to update the model parameters led to the description of these techniques as "iterative methods". Owing to the introduction of a parametrised model, iterative methods are more flexible with respect to direct ones, as confirmed by many successful applications to heritage buildings (e.g. Bonato et al., 2000; Gentile et al., 2017; Pau & Vestroni, 2008; Ceravolo et al., 2016). However, MMU for large and complex structures typically requires local or global sensitivity calculations on the parameters to reduce the computational problems (Mottershead & Friswell, 1993; Bursi et al., 2014; Boscato et al., 2015).

In recent years, the iterative MMU has undergone many computational improvements. For instance, Li & Hong (2011) presented an iterative model updating with a model reduction technique. Their method reduced the undesirable effects of the model reduction process by adding a correction term to the optimisation algorithm. Shan et al. (2016) proposed a stiffness variation-based stabilising objective to be incorporated into iterative optimization with the classical

performance objectives to improve the model feasibility. As regards iterative probabilistic model updating, Sun & Betti, 2015, proposed a hybrid (swarm-based) optimisation algorithm and a regularized objective function derived from Bayesian inference.

Iterative methods can be advantageously used also for MultiPhysics Updating (MPU), i.e. a method that uses experimental data from various physical fields (Humbert et al., 1999). MPU methods can be divided in coupled and uncoupled approaches. The coupled approach involves the use of a coupled multiphysics model containing degrees of freedom related to all the physical fields considered for the analysis, such as thermal, electrical or mechanical.This approach is advantageous when the interaction between the different fields is strong and for analysing non-linear problems (Link and Zimmerman, 2007). Conversely, the uncoupled approach can be used when the different physical fields do not exhibit any important interaction.

The choice of the type of experimental data to be used in the MPU is crucial, also in terms of cost effectiveness. For instance, temperature data are often available, mainly due to the low cost of thermometers and the ease of installation of the monitoring setup.

In the present paper, an iterative MPU methodology for uncoupled multiphysics models is proposed and applied to a large and complex monumental building. This scheme,is complemented, in the iterative optimisation procedure, by a novel metaheuristic approach with random generation of parameters, which avoid instabilisation of parameter estimation in the cycles. By means of the developed algorithm it proves possible to obtain high efficiency and accuracy in the calibration of computationally demanding models, like those typically used for heritage structures.

In more detail, in Section 2 the thermo-mechanical model updating methodology is presented, with a focus on: (i) the general computational scheme; (ii) the metaheuristic algorithm and (iii) the cost function. With this approach, the elastic properties of a structure are obtained from the interaction between a thermal and a mechanical analysis. In Section 3 the methodology is applied to the case study of the Sanctuary of Vicoforte, the historical building that contains the world's largest masonry oval dome.

The results of the thermo-elastic FE model updating applied on the case study are presented and discussed in the final subsection.

2 THERMO-ELASTIC MODEL UPDATING

The classical formulation of thermoelasticity was consolidated in the second half of the last century, thanks to the contribution of scientists like Biot (1956), Boley & Weiner (1960), Parkus (1968), Nowinski (1978). This thermoelasticity theory was then extended to solve the paradox of the infinite speed of heat propagation, bringing to the current formulation of generalised thermoelasticity (Lord & Shulman, 1967; Green & Lindsay, 1972; Szekeres, 1980). Nowadays, this theory is being extended to consider non-linear structures and materials (Kiani & Eslami 2016; Kiani & Eslami, 2017, Kazemnia Kakhkia et al., 2016).

2.1 Thermoelasticity equations

In linear thermoelasticity, the mechanical and thermal fields are coupled through the classical equations (e.g. Balla, 1989):

$$\mu\,\nabla^2\boldsymbol{u} + (\lambda + \mu)\,\nabla(\nabla\cdot\boldsymbol{u}) + \beta\,\nabla Y + \rho\,\boldsymbol{F} - \rho\,\ddot{\boldsymbol{u}} = 0 \tag{1a}$$

$$K_c\,\nabla^2 Y - \rho c\,\dot{Y} + \rho N + \beta T_0\,(\nabla\cdot\dot{\boldsymbol{u}}) = 0 \tag{1b}$$

where: $\boldsymbol{u}$ are the displacements; $\boldsymbol{F}$ are the external forces per unit mass; λ and μ are the Lamé's constants; ρ is the mass density; β is the thermal modulus; K_c is the thermal conductivity; c is the specific heat per unit mass; N is the strength of the internal heat source per unit mass; T_0 is the initial temperature; Y is the temperature difference from T_0; finally, ∇, $\nabla\cdot$ are the spatial gradient and divergence operators, while ∇^2 denote the Laplacian. The coupled equation of motion, Equation (1a), and the coupled heat-conduction equation, Equation (1b), are achieved from kinematic and constitutive equations.

The coupling between the mechanical and thermal field are given by the third term in Equation (1a) and the fourth in Equation (1b). Consequently, apart from the case in which the initial temperature coincides with the absolute zero, the two fields can be completely uncoupled if the thermal modulus β of the material tends to zero. Instead, if the distribution of the temperature inside the body is uniform, the third term in Equation (1a) goes to zero and the linear effect of the spatial gradient of the temperature on the equations of motion vanishes. Conversely, when a spatial gradient of the displacement rate in Equation (1b) can be excluded, the mechanical problem will not affect the thermal one. In this case it is possible to integrate Equation (1b) and find the temperature distribution Y, which can be applied in a second step to Equation (1a). This results in a partially uncoupled approach, that can be followed to update the model through an iterative process. In other words, in a recursion, the results of the thermal model are used as input for the mechanical one. The linear effect of the temperature field on the mechanical response is still considered thanks to the existence of the third term in Equation (1a).

2.2 Methodology for the thermo-mechanical model updating

The proposed model updating methodology is based on the thermoelasticity Equations (1), thus coming down to a thermo-elastic updating, and implies a recursive process to uncouple their resolution.

The flowchart reported in Figure 1a depicts the holistic MPU methodology. The first two steps are the Mechanical Modal Updating (MeMU), that in this study is represented by an MMU, and the Thermal Model Updating (TMU) (Peeters et al., 2015; Sun et al., 2015; Yuan et al.2018), respectively. The MeMU is used to calibrate the mechanical properties of the FE model from the observed dynamic behaviour of the structure. On the other hand, the TMU is used to calibrate the thermal parameters of the structure and/or to determine the temperature distributions within the structure. If the thermal parameters are known, the TMU will reduce to a simple Thermal Analysis (TA) and, consequently, the TA will provide only the temperature distributions. The TMU or TA may relate to the whole model or a portion of it. This latter case holds, for example, when the thermal response of the portion being analysed is not appreciably influenced by the rest of the modelled structure, thus producing a benefit in terms of computational time. In an analogous way, the TMMU can be extended to the entire model or can involve just a part of it.

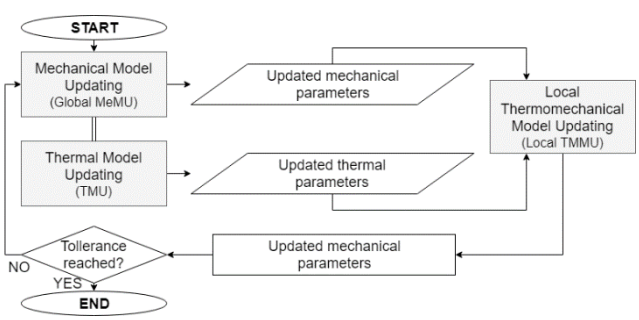

(a)

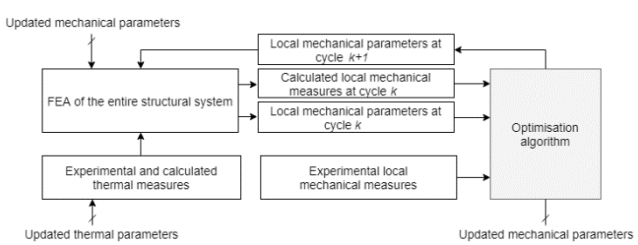

(b)

Figure 1. Holistic methodology for the MPU (a), and local TMMU scheme (b); k denotes the index of a generic cycle of the calibration.

Only the parameters affected by the temperature are calibrated as part of the TMMU. As a consequence, the number of updating variables decreases.

It is worth noting that a more general updating procedure might take into account other sources of data, if available, to improve the reliability of the results, such as data coming from crack-meters, pressure cells, wire gauges, piezometric electric cells, hydrometers, etc.

The TMMU scheme in Figure 1b this time applies to the FEM subjected to the previously calculated thermal distribution.

The TMMU receives as input the mechanical parameters coming from the MeMU and the thermal distribution obtained by the TA, and supplies as output the static response (e.g. reaction forces). The optimisation of the elastic parameters of the partial model entails the reduction of the difference between the numerical static response and the measured one (force measured by the load cells).

2.3 Optimisation algorithm

Countless number of algorithms have been developed in the past for any kind of optimisation. Algorithms inspired by natural phenomena have been manifold in many applications due to their versatility (Nazmul & Adeli, 2016). In the field of civil engineering the interested applications range from infrastructure (Cow, 2014), to structural engineering, including more specialised fields such as control engineering (Jiang & Adeli, 2008).

Among many viable optimisation strategies, based for example on genetic algorithms (Sarma & Adeli, 2006), or more in general evolutionary systems (Siddique & Adeli, 2013), the proposed optimisation algorithm is characterised by the use of a linear mapping between the experimentally identified quantities (e.g. modal frequencies and shapes) and the numerical parameters (e.g. elastic moduli of the FE), avoiding any local approximation, such as approximations with partial derivative of the model parameters (output) with respect to the experimental quantities (input) (Mottershead et al., 2011).

Thus, the main assumption of this method regards the definition of a projection matrix that is computed at each optimisation cycle, *k*, by multiplying two matrices. The first one is a rectangular matrix that contains in the columns the vectors of the past estimates for the numerical or model parameters. The second one is a square matrix and is the inverse of a matrix having in the columns the vectors of the past estimates of the modal quantities supplied by the FE model.

The inversion is performed through the Singular Value Decomposition (SVD). Using the SVD the projection matrix is updated at each cycle for the estimation of the next set of model parameters.

In general, indicating with *p* and *m* the number of model parameters and modal quantities, respectively, and being $\boldsymbol{\theta} \in \mathbb{R}^{px1}$ and $\boldsymbol{\zeta} \in \mathbb{R}^{mx1}$ the corresponding vectors, the projection matrix, ${}^{k}\bar{\boldsymbol{R}}$, can be written as:

$$ {}^{k}\bar{\boldsymbol{R}} = {}^{k}\boldsymbol{\Theta}\ {}^{k}\boldsymbol{Z}^{\dagger} \tag{2} $$

where ${}^{k}\boldsymbol{\Theta} \in \mathbb{R}^{pxn}$ contains the column vectors ${}^{k}\boldsymbol{\theta}$ of the *n* past estimates of the model parameters resulting from the calibration (i.e. ${}^{k}\boldsymbol{\Theta} = [{}^{k-n+1}\boldsymbol{\theta} \ldots {}^{k-1}\boldsymbol{\theta}\ {}^{k}\boldsymbol{\theta}]$), while ${}^{k}\boldsymbol{Z}^{\dagger}$ is the pseudo-inverse matrix of ${}^{k}\boldsymbol{Z}$, computed through the SVD

algorithm. ${}^{k}\boldsymbol{Z} \in \mathbb{R}^{mxn}$ contains the column vectors ${}^{k}\boldsymbol{\zeta}$ of the n past estimates of the modal quantities supplied by the FE model (i.e. ${}^{k}\boldsymbol{Z} = [{}^{k-n+1}\boldsymbol{\zeta} \dots {}^{k-1}\boldsymbol{\zeta}\ {}^{k}\boldsymbol{\zeta}]$).

In order to improve the stability of the algorithm, the parameter n is selected to obtain a square matrix, ${}^{k}\boldsymbol{Z}$, thus imposing n=m. The model parameters in the successive cycle are then evaluated as:

$$ {}^{k+1}\boldsymbol{\theta} = {}^{k}\overline{\boldsymbol{R}}\ {}^{id}\boldsymbol{\zeta} \tag{3} $$

where ${}^{id}\boldsymbol{\zeta}$ is the vector of the experimental data.

When performing a MMU, the experimental data are typically modal frequencies ${}^{id}f_j$ and modal shapes, the latter in the form of Modal Assurance Criterion, ${}^{k}MAC_j$. As for the cost function, ${}^{k}J({}^{k}\boldsymbol{\theta})$, in this study it is assumed as follows (Merce et al., 2007; Moller et al., 1998):

$$ {}^{k}J({}^{k}\boldsymbol{\theta}) = = \sum_{j=1}^{m} \alpha_w \left(\frac{{}^{id}f_j - {}^{k}f_j}{{}^{id}f_j} \right)^2 + \beta_w \left(\frac{1 - \sqrt{{}^{k}MAC_j}}{{}^{k}MAC_j} \right)^2 \tag{4} $$

where α_w and β_w are the weights of the squared difference between ${}^{k}\zeta_j$ (i.e. numerical frequencies, ${}^{k}f_j$, and the square root of the MAC between the numerical and experimental modes, ${}^{k}MAC_j$) and ${}^{id}\zeta$ (i.e. experimental frequencies, ${}^{id}f_j$, and the ideal MAC, i.e. equal to 1), respectively.

For the TMMU, ${}^{id}\zeta$, are the loads in the tie-bars recorded by the load cells and ${}^{k}\zeta_j$, are the corresponding numerical values supplied by the model. The cost function in this case has the same structure as that expressed in Equation (4), but the vector of experimental data, ${}^{id}\zeta$, will be the loads in the tie-bars recorded by the load cells and ${}^{k}\zeta_j$, are the corresponding numerical values supplied by the model.

The recursive procedure continues until the following criterion is satisfied:

$$ \left| {}^{max,k}\boldsymbol{g} - {}^{min,k}\boldsymbol{g} \right| < \tilde{\boldsymbol{\varepsilon}} \tag{5} $$

where $\tilde{\boldsymbol{\varepsilon}}$ is a maximum accepted deviation and ${}^{max,k}\boldsymbol{g}$ and ${}^{min,k}\boldsymbol{g}$ defines the normalised range of generation of the model parameters.

In fact, the model parameters, ${}^{k}\boldsymbol{\theta}$, need to be randomly re-initialised when they reach the normalised boundaries of the variation range $[{}^{min}\boldsymbol{\theta}_n; {}^{max}\boldsymbol{\theta}_n]$, in order to avoid instability in the process. More specifically, during the optimisation the range of random generation of parameters progressively change according to the following laws:

$$ {}^{min,k}\boldsymbol{g} = \frac{{}^{min}J}{{}^{0}J}\,{}^{min,(k-1)}\boldsymbol{g} + \left(1 - \frac{{}^{min}J}{{}^{0}J}\right){}^{id}\boldsymbol{\theta}_n \tag{6a} $$

$$ {}^{max,k}\boldsymbol{g} = \frac{{}^{min}J}{{}^{0}J}\,{}^{max,(k-1)}\boldsymbol{g} + \left(1 - \frac{{}^{min}J}{{}^{0}J}\right){}^{id}\boldsymbol{\theta}_n \tag{6b} $$

where ${}^{min}J$ and ${}^{0}J$ are the smallest and the initial value of the cost function and ${}^{id}\boldsymbol{\theta}_n$ is the vector of the normalised parameters associated to ${}^{min}J$. For $k = 1$, ${}^{min,0}\boldsymbol{g}$ and ${}^{max,0}\boldsymbol{g}$ are assumed equal to ${}^{min}\boldsymbol{\theta}_n$ and ${}^{max}\boldsymbol{\theta}_n$, respectively.

The normalised i-th parameter at cycle k, ${}^{k}\theta_{n,i}$, is defined as:

$$ {}^{k}\theta_{n,i} = \frac{{}^{k}\theta_i - {}^{min}\theta_i}{{}^{max}\theta_i - {}^{min}\theta_i} - \frac{1}{2} \tag{7} $$

where ${}^{min}\theta_i$ and ${}^{max}\theta_i$ identify the not-normalised boundaries of the variation range of the i-th parameter ${}^{k}\theta_i$, that fill the vector ${}^{k}\boldsymbol{\theta}$.

During the process, the normalised range of generation $[{}^{min,k}\boldsymbol{g}; {}^{max,k}\boldsymbol{g}]$ tends to narrow around ${}^{id}\boldsymbol{\theta}_n$, until ${}^{min,k}\boldsymbol{g}$ becomes equal to ${}^{max,k}\boldsymbol{g}$, with a tolerance $\tilde{\boldsymbol{\varepsilon}}$. Consequently, even if the normalised parameters are in the range $[{}^{min}\boldsymbol{\theta}_n; {}^{max}\boldsymbol{\theta}_n]$, the random re-initialisation will fall inside $[{}^{min,k}\boldsymbol{g}; {}^{min,k}\boldsymbol{g} + \tilde{\boldsymbol{\varepsilon}}]$, and the optimisation will go to convergence when Equation (5) is satisfied. Thus, the optimality condition is ruled by the random re-initialisation of the normalised model parameters around ${}^{id}\boldsymbol{\theta}_n$.

The described improvement (random generation of parameters) leads to a reduction of iterations to 1/10 - 1/100 with respect to standard heuristic algorithms (e.g. genetic algorithm, particle swarm etc.). Thus, with this metaheuristic algorithm high efficiency and accuracy can be obtained in the calibration of computationally demanding models, like those used to simulate heritage structures.

3. THERMO-ELASTIC MODEL UPDATING OF THE WORLD'S LARGEST OVAL MASONRY DOME

The Sanctuary dedicated to Regina Montis Regalis is a monumental masonry building located in Vicoforte, Italy (Figure 2). The construction began in 1596 and finished in 1735. The impressive oval dome is the fourth largest masonry dome in the world and the world's largest oval one, with internal axes of 37.23 by 24.89 meters (Chiorino et al. 2006; Chiorino et al., 2008) (Figure 3).

Since the first years of its construction, the building has been affected by several structural problems due to the differential settlement caused by the heterogeneous characteristics of the soil underlying the foundation

(Casalegno et al., 2014). In 1987 a strengthening system, consisting of 4 rings composed by 56 active steel tie-bars, was put in place at the drum level in order to reduce the horizontal cracks. In the same year, a static monitoring system was designed and installed (Chiorino et al., 2008).

To better understand the structural behaviour of the Sanctuary, several non-destructive survey campaigns have been conducted during the last few decades (Aoki et al., 2004), and a first dynamic testing campaign was performed in 2008 (Chiorino et al., 2011). More recently, the data acquired by the static monitoring system, in the decade 2004-2014, underwent a systematic analysis that proved the cracks had not widened and, therefore, the effectiveness of the strengthening system put in place in 1987 (Ceravolo et al., 2017).

In 2016 a permanent dynamic and seismic monitoring system was installed to investigate the global phenomena affecting the structure (Pecorelli et al., 2017). The continuous monitoring permits to appreciate seasonal variations of modal parameters. Hence, the results of the model calibration performed on these new records have a higher statistical significance with respect to previous campaigns.

The dynamic parameters identified using the records acquired from 2016 onwards substantially confirmed the main modes identified during the dynamic tests carried out in 2008 (Chiorino et al., 2011). This result, combined with the systematic analysis of the data acquired by the static monitoring system, suggests that no important damage progression has occurred in the last decade. Consequently, the information supplied by the dynamic monitoring system can be combined with data acquired by the static monitoring one, in spite of being referred to different periods.

The numerical FE model developed for the Sanctuary is composed by spring, link, beam, shell and brick elements, for a total of about 210228 elements and 119192 nodes. The average dimension of the mesh is about 0.8 m and varies from the soil to the lantern.

Figure 2. External view of the Sanctuary of Vicoforte.

3.1 The model updating methodology

The MPU procedure, as proposed in Section 2, has been further articulated and implemented for application to large and complex monumental buildings, such as the Sanctuary of Vicoforte.

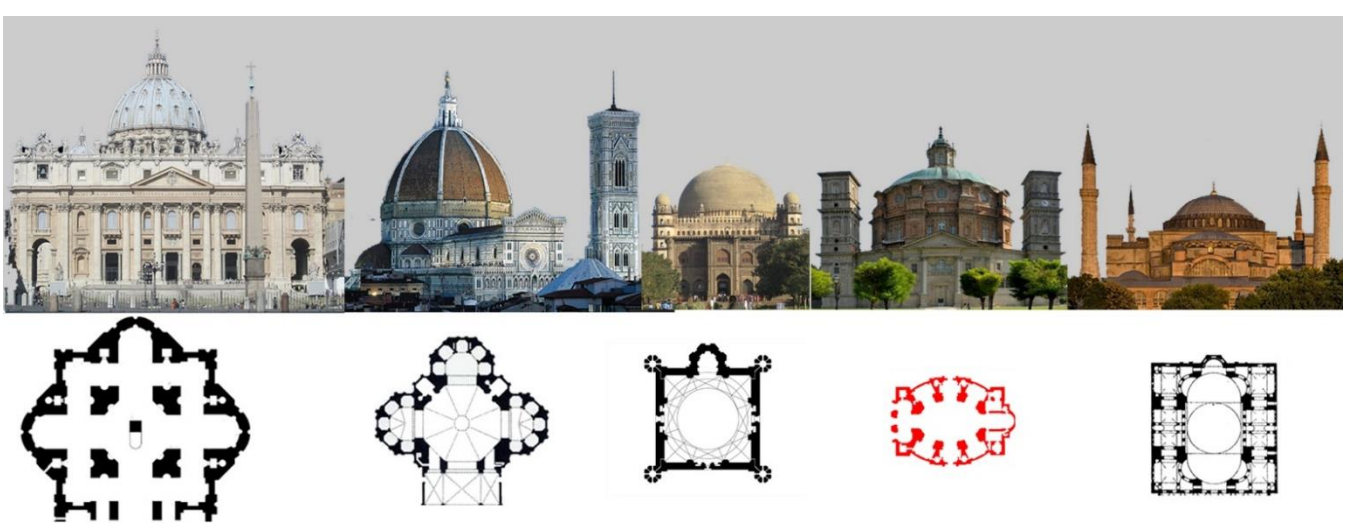

Figure 3: Ranking of the world's largest masonry domes.

In detail, the application of the methodology can be summarised in four steps: (i) preliminary dynamic model updating of the entire model (reference starting configuration); (ii) thermal analysis on a portion of the model (partial model); (iii) TMMU of a portion of the model; (iv) MMU of the entire model. Figure 4 reports a layout of the methodology with the different steps.

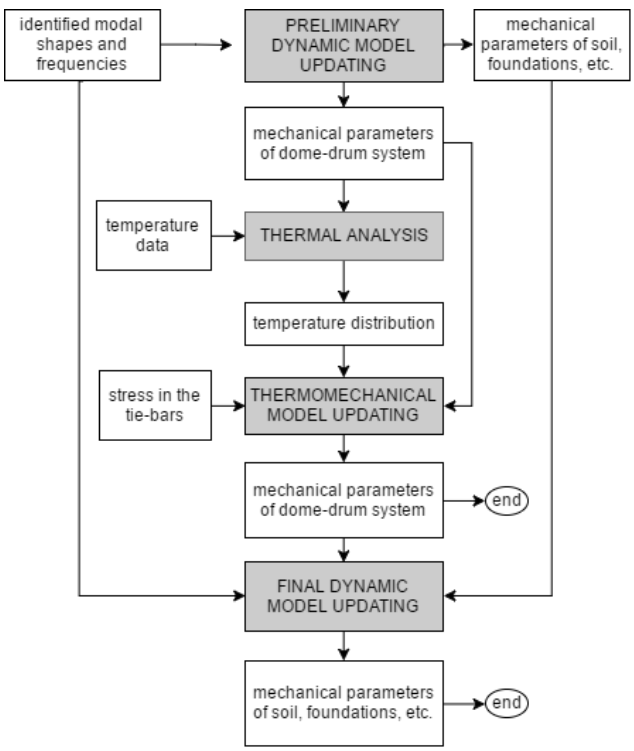

Figure 4. Layout of the methodology.

The preliminary model updating, based on the experimental modal parameters, provided a first estimate of the mechanical parameters for all the macro-elements (dome, drum, buttresses, basement, bell towers, tie-bars, clay, marlstone and lantern) of the FE model. The elastic parameters obtained by the preliminary model updating were used in the local thermal analysis of the drum-dome system. Then, the temperature data recorded in a finite number of points were used in the thermal model to extrapolate the temperature distribution of the drum-dome system. It is worth noting that, according to this procedure, the thermal and the mechanical analyses are partially decoupled in the assumption of a uniformly zero velocity field (see Equation (1b) for clarity).

The aim of this updating was to obtain the values of the elastic parameters that best reproduce the tensile forces measured in the hooping system. The updating can be restricted to the drum-dome system because, in this model, the forces in the tie-bars are not significantly affected by the thermal behaviour of the omitted macro-elements.

Thus, the TMMU process consisted in minimising the difference between the measured and numerical forces in the tie-bars, under the calculated thermal distribution. At the end of the procedure, the elastic parameters of the drum-dome system were updated.

Since the model used in the TMMU simulates only a part of the structure, the assimilation of the new parameters into the global model hardly can result in a perfect fitting in terms of modal parameters. Consequently, a further dynamic model updating was required. However, in this last calibration, the elastic parameters of the drum-dome system were kept fixed and the updating involved the other portions of the structure. In fact, the global vibration modes are not very sensitive to the elastic parameters of the drum-dome portion.

It is worth underlining that in the general case the holistic TMMU should extend to all macro-elements, and a recursive procedure between the TMMU and the MMU should be activated in order to obtain more accurate results.

3.2 Preliminary model updating

The first model updating of the Sanctuary was performed by Chiorino et al., 2011, and was based on the results of a dynamic test campaign conducted in 2008. The campaign consisted of 7 different setups, each one of 12 accelerometers mainly located in correspondence of the dome. Modes were identified essentially from ambient vibration records. Figure 5 reports three of the measurement setups.

This first updating relied on a homogeneous model, that did not account for different types of materials. Even soil-structure interaction had been neglected. In fact, this calibration was essentially aimed to support the identification of higher modes whose classification was uncertain.

The geometric and mechanical models of the Sanctuary exploited multi-disciplinary information gathered with laser scanner survey, historical documentation and geotechnical survey campaigns (Novello & Piumatti, 2012, Aoki et al., 2004).

In particular, the geotechnical investigations revealed the miscellaneous composition of the soil underlying the building: a marl layer slants downward from the north-east to the south-west corner (dip angle 5°- 6°), whilst under the rest of the building there is a clay layer. Therefore, three of the eight pillars are based on a marl layer while all the others float on the clay layer. Details on cross-hole tests–are reported in Chiorino et al., 2008, and Casalegno et al., 2014.

Successively, in order to consider the structural, typological and historical peculiarities of each component of the structure, a more accurate FE model was built that consisted of 9 homogeneous macro-elements: 7 for the building (lantern, dome, drum, basement, buttresses, bell-towers and iron ties) and 2 for the soil (marl and clay), see Figure 6 for clarity.

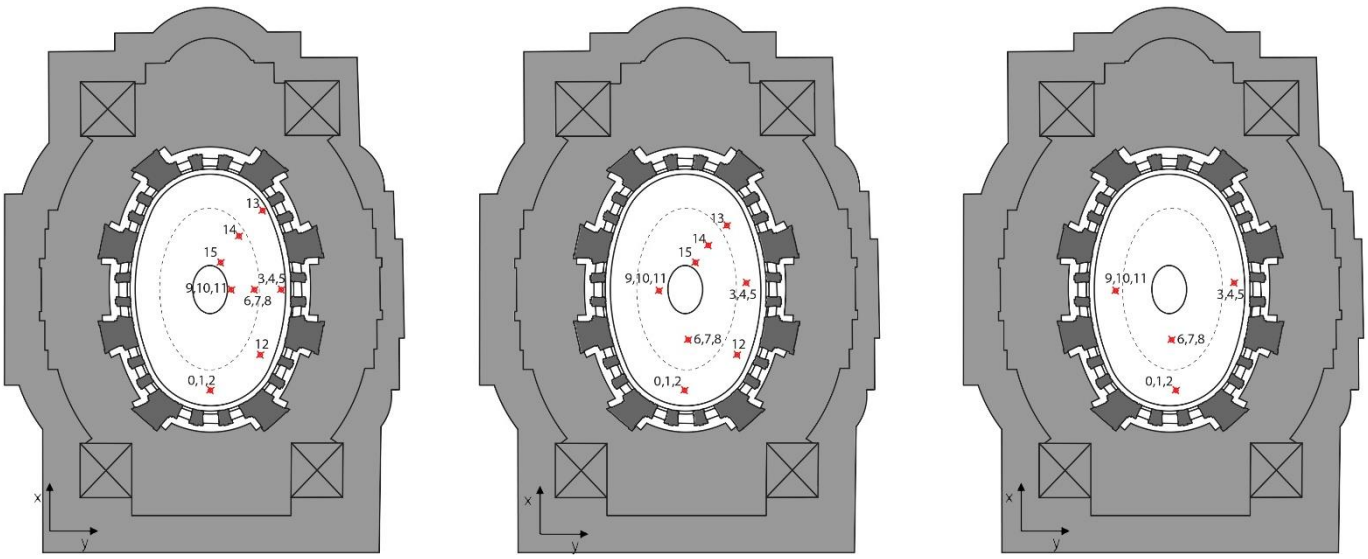

Figure 5. Three of the setups used in the dynamic test campaign of the 2008.

Most of the structure was modelled by 8-node brick elements, in consideration of their volumetric and spatial complexity (Casalegno et al. 2014). Instead, shell elements were used to model the lantern, the bell-towers, the buttresses, the thin vaults of the radial chapels, the apse, the atrium and the dome (Ceravolo et al. 2016). The cracking pattern, located especially in the drum-dome area, was taken into account in the process by reducing Young's modulus of the cracked macro-elements. The bottom part of the FE model (soil, foundations and pillars) was modelled using 8-node hexahedral solid elements. A weak interaction between the Sanctuary and the adjoining convent building was modelled through spring elements.

The initial values of the masonry properties were assigned in accordance with the experimental data obtained by non-destructive tests carried out in 2004 (Aoki et al., 2004). The elastic moduli resulting from this test campaign spanned from 1.3 to 4.8 GPa and the average Poisson's ratio was about 0.38.

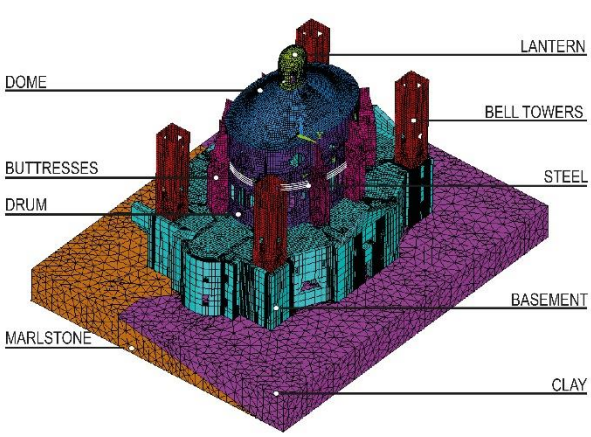

Figure 6. The FE model of the Sanctuary.

The preliminary calibration followed a multi-step procedure based on the first five modes, among those identified after the 2008 dynamic campaign (Casalegno et al. 2014). In this calibration, the cost function of Equation (4) was minimised in accordance with previous studies (Merce et al. 2007; Ceravolo et al., 2014). The weighting coefficients for frequency and modal shapes were kept constant to 1.

Table 1 reports the mechanical characteristics of the macro-elements at the end of the preliminary calibration, which involved the elastic moduli, the Poissons' coefficients and the mass density of all the macro-elements. However, the successful calibration process does not imply that the model is locally verified. This is particularly true for macro-elements whose dynamics is ruled by local modes, such as the drum-dome system.

Table 1
Values of the mechanical parameters after the preliminary calibration

Macro-element	*E (GPa)*	*υ (-)*	*ρ (Kg/m³)*
Bell-towers	2.00	0.35	1800
Basement	2.90	0.35	1800
Buttresses	2.70	0.30	1700
Clay	0.55	0.35	1900
Dome	5.90	0.35	1800
Drum	2.60	0.30	1700
Lantern	1.80	0.35	1800
Marlstone	4.15	0.35	2100
Steel	210	0.30	7800

3.3 Thermal analysis

The aim of the thermal analysis is to obtain the temperature distribution of the drum-dome system as related to the forces acting in the tie-bars. This distribution was determined by applying local temperature measurements to the thermal FE model. The temperature distribution obtained for the drum-dome system was then used as the input for the successive TMMU.

The thermal analysis was performed on the partial FE model of the Sanctuary. In detail, this model was limited to the upper macro-elements: lantern, dome, drum, buttresses, tie-bars (Figure 7). A 4-node shell element was used to model the lantern, the dome, the drum and the buttresses. This is a layered shell element having in-plane and through-thickness thermal conduction capability, suitable for conducting static and transient thermal analysis. The tie-bars of the strengthening system were modelled using 2-node beam elements. Both materials, masonry and steel, were assumed to have isotropic thermal conductivity, as reported in Table 2. In detail, the value for the conductivity parameter, K_c, was assumed to be in accordance with the literature, whilst the mass densities were the same ones used in the preliminary model calibration.

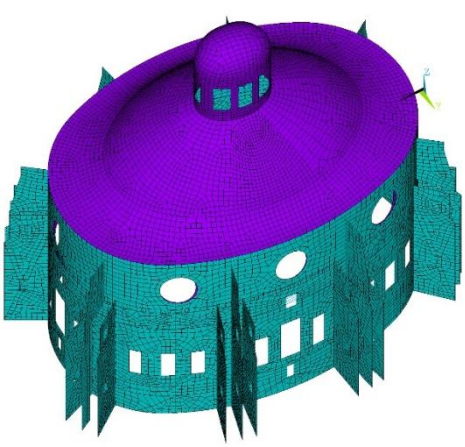

Figure 7. The thermal FE model limited to the upper macro-elements.

Table 2
Thermal and mass properties of the macro-elements

Macro-element	K_c *(W/m·K)*	ρ *(Kg/m^3)*
Buttresses	0.7	1700
Dome	0.7	1800
Drum	0.7	1700
Lantern	0.7	1800
Steel	60.5	7800

The thermal analysis used the brickwork inner temperature defined from the temperature data acquired by the static monitoring system during 2009. Figure 8 shows the positions of the thermometers: internal sensors (T1, T3, T5, T7); external sensors (T2, T4, T6, T8); sensors in the stairwells (T12, T17, T22, T23, T24); sensors on the frames close to the tie-bars (T13-T16, T18-T21); sensors on the extrados of the dome (T9-T11).

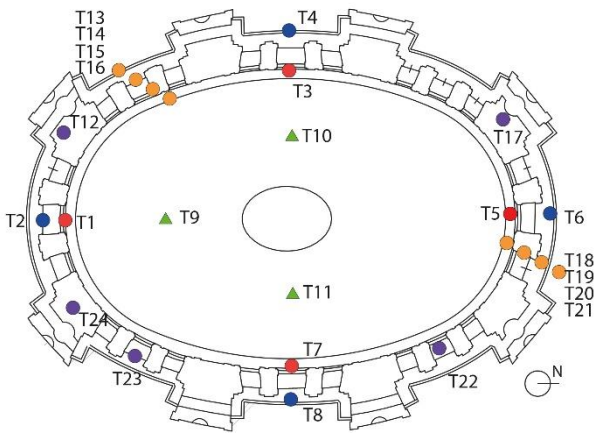

Figure 8. Temperature sensors of the static monitoring system.

In details, the brickwork inner temperature at 32 m and 50 m was defined (i) by calculating the thermal flux q at 30 m, using the internal and the external sensors at this height and then (ii) this value was used to determine the temperature at the mid-thickness of the masonry at 32 and 50 m, starting from the temperature acquired by the internal sensors and by the sensors on the extrados of the dome. The thermal flux, q, was evaluated using the data acquired in winter, when the effects of convention and radiation are negligible.

The data acquired by the sensors on the frames close to the tie-bars (T13-T16 and T18-T21) were not used because previous studies proved that the temperature recorded by these sensors is comparable to the external temperature, due to presence of opening (see Ceravolo et al. 2017). Similarly, the data recorded by the sensors T12, T17, T22, T23 and T24 are not considered as they are located outside the drum-dome system. The brickwork inner temperature was assumed constant along the parallel according to the previous studies (see Ceravolo et al. 2017) which proved that the temperature inside the Sanctuary is constant along the parallel. Defined the temperature time-histories at 32 m and 50 m, the whole temperature distribution was obtained employing FE thermal analysis.

3.4 Thermo-elastic model updating

TMMU was used to calibrate the elastic properties of the partial model, minimising the difference between the

measured and the calculated internal forces in the hooping system.

From a qualitative observation of the static monitoring data, the tensile forces in the tie-bars are seen to decrease during the hot seasons and increase during the cold ones. This behaviour is associated to the different thermal expansion coefficient and thermal inertia of masonry and steel. The validity of the above stated relation for all the tie-bars can be easily proved comparing the temperature measured by the thermometers placed on the tie-bars with the cyclic behaviour of the data acquired by the cell-load sensors. For instance, Figure 9 overlays data trends recorded by the thermometer T20 and the cell load cells LC29 after mean removal (see Figure 8 and Figure 10 for the position of the sensors). This phenomenon results in regular seasonal cycles of the loads in the tie-bars, as reported in Ceravolo et al., 2017. Consequently, the thermo-elastic model can be updated to reproduce the forces measured on the tie-bars when subjected to the temperature distributions recorded over a whole year.

The TMMU of the Sanctuary was thus performed on the partial model derived from the thermal one (shells for masonry and beams for the tie-bars, as for the global model). In order to consider the boundary conditions provided by the missing part of the model (basement, bell-towers and soil) spring elements were introduced at the base of the model. The stiffness of each spring was set to globally reproduce the restoring force applied by the omitted (lower) macro-elements. In particular, the stiffnesses were evaluated on the global model by applying a force field at the base of the drum and reading the displacements in the same nodes. Then, the average value of the stiffness was introduced in the partial model, in the two orthogonal directions.

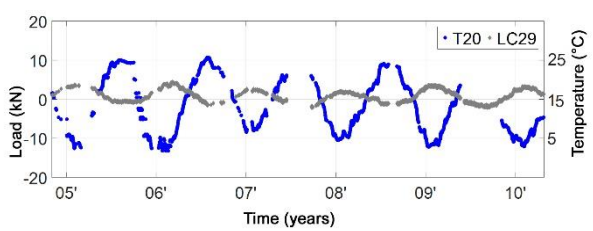

Figure 9. Overlays of the time history of data recorded by the thermometer T20 and the load cell LC29.

The pretension in the tie-bars was modelled applying an axial force to the corresponding elements in the FE model. The initial value of this force, at ambient temperature (i.e. 20 °C), was set equal to the average axial prestress of about 52 MPa evaluated over all the bars (Ceravolo et al., 2017). The hooping system, located in the drum at about 32 m height, was modelled with beams elements and attached to link elements simulating the connection to the masonry.

The TMMU was performed by varying the mechanical parameters of the modelled macro-elements (drum, dome, buttresses and lantern). The cost function used in the optimisation process has the same form of Equation (4), but in this case the measurements vectors, ${}^{k}\boldsymbol{\zeta}$ and ${}^{id}\boldsymbol{\zeta}$, contain the tensile forces in the tie-bars, as the aim of the optimisation is to minimise the difference between the forces obtained with the FE model and the ones measured by the static monitoring system, which are due to the thermal deformation of the structure. In detail, the forces in the tie-bars were measured by load cells placed at the end of each tie-bar of the strengthening system, as shown in Figure 10. The optimisation procedure used data acquired by sensors that showed consistent and reliable behaviour, while data affected by any sort of anomalies (e.g. non-monotonic trends) were discarded (see Ceravolo et al., 2017 for more details). Uniform values equal to 1 were assigned to the weighting coefficients (like in the MMU), in the absence of specific indications.

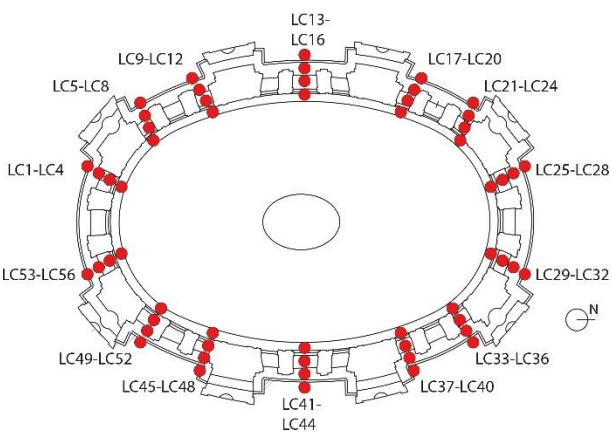

Figure 10. Positions of the load cells.

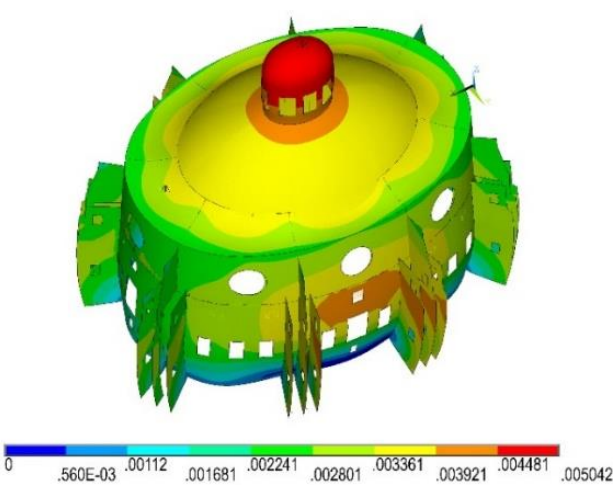

Figure 11. Displacements of the drum-dome system due to a typical temperature distribution in winter (m).

For each set of elastic parameters and temperatures, the displacements of the structure and the forces consequently acting in the tie-bars were calculated. Figure 11 shows, for instance, the displacements of the drum-dome system, during a winter's day, as generated by the temperature distribution resulting from the TA. As it can be seen in Figure 11, the maximum displacements are at the top of the building in correspondence of the lantern.

In Figure 12, the loads measured by the cells LC22 and LC51 (symmetrically located on the West and East side of the strengthening system), and the loads estimated by the model before and after the TMMU are overlaid. Similar trends were also found for other tie-bars.

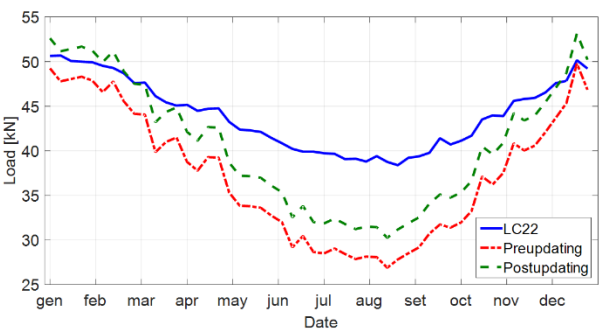

(a)

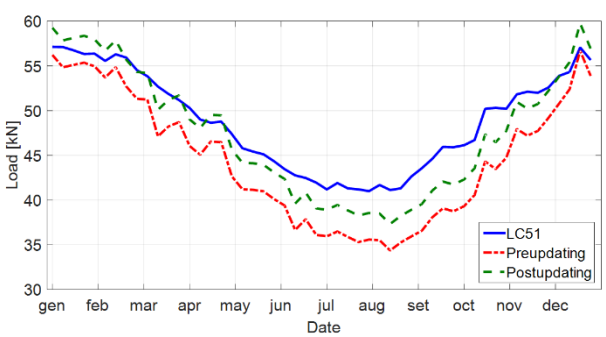

(b)

Figure 12. Pre- and post-updating load trends associated with data acquired by a load cell (a) LC22 and (b) LC51.

Table 3 summarises the mechanical properties of different macro-elements of the partial model before and after the TMMU. With the TMMU the elastic moduli and the Poisson's ratios of the partial FE model were updated. It can be noticed that the elastic properties of the lantern remain unvaried because of the weak interaction of this macro-element with the tie-bars.

As said, updating of the elastic parameters of some macro-elements will result in some modifications in the frequencies of the global model of the Sanctuary. Therefore, a further model updating of the entire model is required to match the experimental frequencies and shapes.

Table 3
Pre- and post-updating values of mechanical properties.

Pre-updating			
Macro-element	*E (GPa)*	*υ (-)*	*ρ (Kg/m³)*
Buttresses	2.70	0.30	1700
Dome	5.90	0.35	1800
Drum	2.60	0.30	1700
Lantern	1.80	0.35	1800
Post-updating			
Macro-element	*E (GPa)*	*υ (-)*	*ρ (Kg/m³)*
Buttresses	**5.50**	0.30	1700
Dome	**5.50**	0.35	1800
Drum	**2.30**	**0.35**	1700
Lantern	1.80	0.35	1800

3.5 Final calibration

The aim of this last calibration step was to restore the capability of the model to describe the dynamic behaviour of the real structure after the TMMU step. To this purpose, only the elastic moduli of the macro-elements that were not taken into account (basement, bell-towers and soil) or that remained unchanged (lantern) in the TMMU, underwent a further updating. The moduli to be updated were initialised to the values found with the preliminary dynamic model updating (see Subsection 3.2). The cost function is still the same of Equation (4), with weighing coefficients kept equal to one. The calibration procedure continues until the stopping criterion reported in Equation (5) is satisfied, assuming the tolerance vector, $\tilde{\boldsymbol{\varepsilon}}$, equal to $10^{-10} \cdot \left|^{min,k}\boldsymbol{g}\right|$.

The experimental modes used for this last calibration were obtained by averaging those identified from data of the permanent dynamic monitoring system over the last year. For details about the dynamic identification procedure one can refer to Pecorelli et al., 2017.

It is worth evidencing that the data of static and dynamic monitoring used in the TMMU refer to different periods, as the dynamic monitoring system was installed more recently. However, this inconsistency is not expected to affect the updating as no important changes in the static or dynamic behaviour were recorded over the last decade. In particular, modal quantities identified in 2017 were used in this last updating.

The first three modes (1st bending Y, 1-st bending X, and 1-st torsional, in terms of frequencies and MAC) were used to update the 5 elastic moduli of basement, bell-towers, clay marlstone and lantern, respectively. With this configuration, the number of parameters to be optimised resulted lower of the available experimental data (3 frequencies and 3 MAC), this also thanks to the previous TMMU. At the end of the calibration, the vibration modes of the updated model are

seen to be in good agreement with the experimental ones, both in terms of frequencies and modal shapes. In more detail, it can be noted from Table 4 that for the first three frequencies the error is lower than 1%, with a perfect matching for the 1st bending in Y direction and for the torsional one. The MAC between experimental and updated modal shapes, as presented in Figure 13b, confirms the good correspondence between the updated model and the monitoring data. At the same time, also the static behaviour, in terms of stress in the tie-bars, shows a good correspondence, as a result of the TMMU step. It is also possible to notice (see Table 5 and Table 6), that the calibrated value of the Young's modulus of the basement and drum regions is around 2 GPa, while higher values, about 5 GPa, are found for the other macro-elements. This is confirmed by the literature values (Aoki et al., 2004) and by the pronounced and distributed cracking pattern observed in the drum region.

Table 4
Experimental frequencies identified from data of the permanent monitoring system (averaged over a year) and numerical frequencies.

Reference values		*Preliminary updating*		*Final updating*	
Mode	f_{ID} *(Hz)*	f_{FEM} *(Hz)*	*Error (%)*	f_{FEM} *(Hz)*	*Error (%)*
1st bending Y	1.93	1.98	0.50	1.93	0.00
1st bending X	2.09	2.20	-5.77	2.11	-0.96
1st torsional	2.84	2.98	12.87	2.84	0.00
2nd bending Y	3.60	4.00	-29.87	3.89	-8.06
2nd bending X	3.96	4.29	-13.79	4.17	-5.30

Figure 14 reports the first three modal shapes of the Sanctuary as resulting from the proposed updating procedures, while Table 5 summarises the corresponding elastic parameters at the end of the process.

As already stated in Section 3.1, in the general case, the holistic TMMU should extend to all macro-elements, and a recursive procedure between the TMMU and the MMU should be activated.

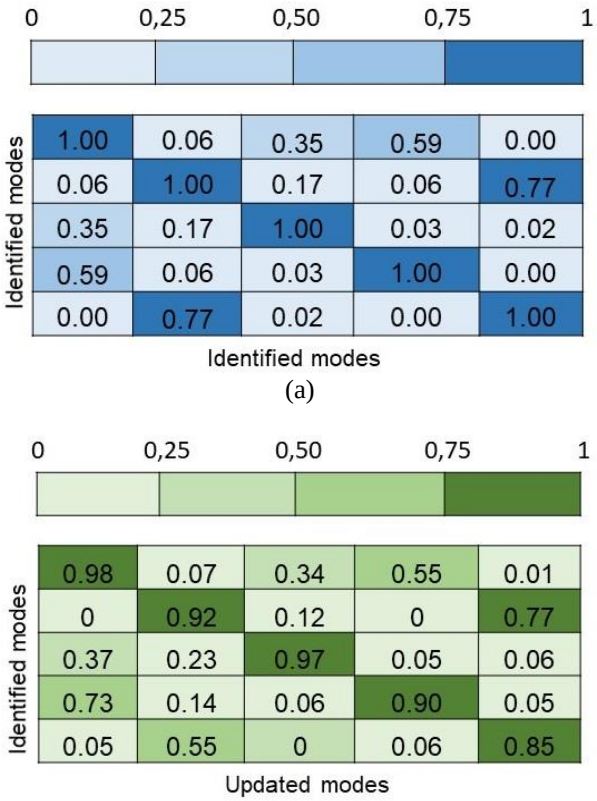

Figure 13. MAC obtained using only the experimental modes (a); MAC between experimental and updated numerical modal shape (b).

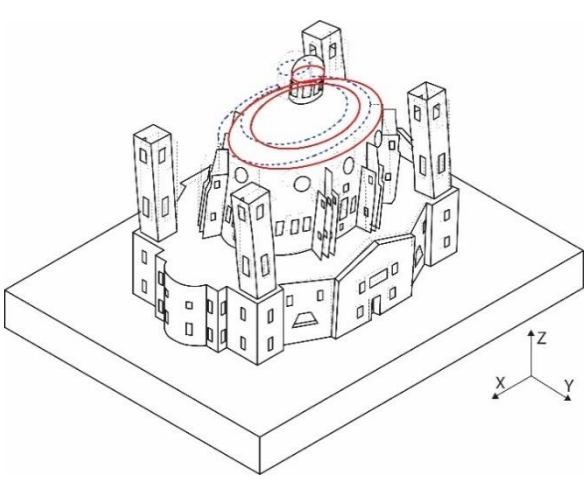

(a)

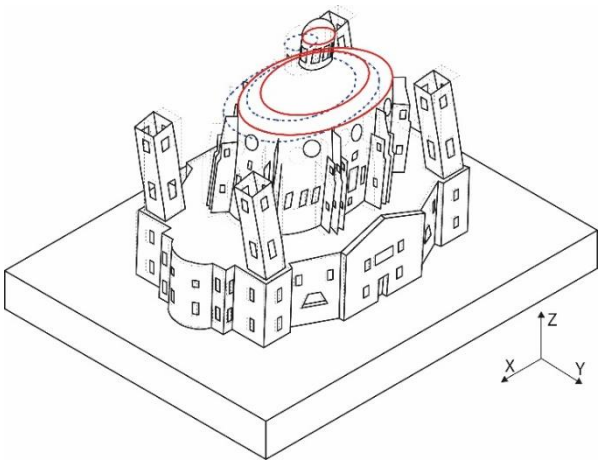

(b)

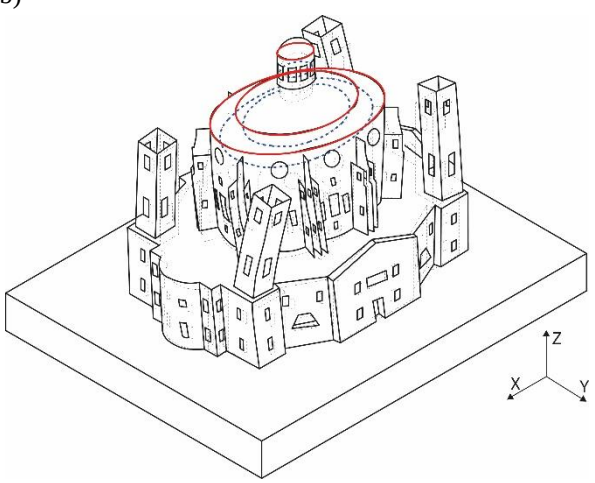

(c)

Figure 14. First three modal shapes of the Sanctuary of Vicoforte: (a) 1-Y, (b) 1-X, (c) 1-T. Dotted lines identify the undeformed configuration at the dome level.

Table 5
Values of the elastic moduli after the final calibration.

From the thermo-mechanical model updating			
Macro-element	*E (GPa)*	*ν (-)*	*ρ (kg/m³)*
Buttresses	5.50	0.30	1700
Dome	5.50	0.35	1800
Drum	2.30	0.35	1700
From the final dynamic model updating			
Macro-element	*E (GPa)*	*ν (-)*	*ρ (kg/m³)*
Bell-towers	4.50	0.35	1800
Basement	2.00	0.35	1800
Clay	0.75	0.35	1900
Lantern	5.60	0.35	1800
Marlstone	5.00	0.35	2100

Table 6
Comparison between preliminary (*pre.*) and final (*fin.*) elastic parameters.

Macro-element	*E (GPa)*		*υ (-)*		*ρ (Kg/m³)*	
	pre.	*fin.*	*pre.*	*fin.*	*pre.*	*fin.*
Bell-towers	2.00	**4.50**	0.35	0.35	1800	1800
Basement	2.90	**2.00**	0.35	0.35	1800	1800
Buttresses	2.70	**5.50**	0.30	0.30	1700	1700
Clay	0.55	**0.75**	0.35	0.35	1900	1900
Dome	5.90	**5.50**	0.35	0.35	1800	1800
Drum	2.60	**2.30**	0.30	**0.35**	1700	1700
Lantern	1.80	**5.60**	0.35	0.35	1800	1800
Marlstone	4.15	**5.60**	0.35	0.35	2100	2100
Steel	210	210	0.30	0.30	7800	7800

In Table 6 a comparison between the preliminary and the updated elastic parameters is reported. From this table it can be observed that after the calibration process significant changes occurred in the elastic properties of many of the macro-elements relative to the preliminary model updating. This is visible also by looking at the Young's modulus of the buttresses before and after the calibration. Its value changed about of about 100% after the updating conducted with local thermo-elastic data, i.e. temperatures and internal forces in the tie-bars. Finally, it is worth noting that also the bell-towers underwent important changes after calibration. Nevertheless, due to lack of direct measurements on these elements, the final updating for bell-tower macro-elements is deemed less reliable. Opposite is the case of the lantern, whose elastic modulus is seen to triplicate after the last updating. This difference can be associated to the fact that this macro-element had not been instrumented in the first dynamic test campaign.

4. CONCLUSIONS

This paper combines dynamic and thermo-elastic model updating for the calibration of elastic properties in complex FE models, like those used to simulate the structural behavior of monumental structures. Moreover, in order to obtain the required efficiency for updating such computationally demanding models, a novel metaheuristic approach with random generation of parameters has been introduced.

The whole methodology has been demonstrated on a large and complex monumental building, i.e. the Sanctuary of Vicoforte, based on data from both static and dynamic monitoring systems, and exploiting the information related to the cyclic seasonal behavior of masonry and steel elements.

The results obtained in this research show that the proposed multiphysics approach can introduce significant

improvements in the accuracy of complex FE models, thus producing real predictions of both static and dynamic behaviors.

In conclusion, to the authors' knowledge, this study constitutes the first example of thermo-mechanical model updating applied to an important monumental building, namely the world's largest masonry oval dome.

Future studies on the Sanctuary of Vicoforte will take advantage of the thermo-elastic model in order to predict the wandering of modal parameters. This will require further investigations on the role played by the soil-structure interaction. In addition, a study on the sensitivity of the modal and thermal analysis with respect to the basic variables of the identification problem will be performed to increase the reliability of the calibration process and the accuracy of the results, especially as regards the tie-bars forces.

References

Aoki, T., Komiyama, T., Tanigawa, Y., Hatanaka, S., Yuasa, N., Hamasaki, H., Chiorino, M. A. & Roccati, R. (2004), Non-destructive testing of the sanctuary of Vicoforte, *Proc. 13th International Brick and Block Masonry Conference*,Amsterdam, July 4-7.

Balla, M. (1989), Formulation of coupled problems of thermoelasticity by finite elements, *Periodica Polytechnica Mechanical Engineering*, **33**(1-2), 59-70.

Biot, M. A. (1956), Thermoelasticity and Irreversible Thermodynamics. *Journal of Applied Physics*, **27**, 240-253.

Boley, B. A. & Weiner, J.H. (1960), Theory of Thermal Stresses. J Wiley and Sons, New York.

Bonato, P., Ceravolo, R., De Stefano, A. & Molinari, F. (2000), Cross-Time Frequency Techniques for the Identification of Masonry Buildings, *Mechanical Systems And Signal Processing*, **14**,91-109.

Boscato, G., Russo, S., Ceravolo, R. & Zanotti Fragonara, L. (2015), Global Sensitivity-Based Model Updating for Heritage Structures, *Computer-Aided Civil and Infrastructure Engineering*, **30**(8), 620-635.

Bursi, O.S., Kumar, A., Abbiati, G. & Ceravolo, R. (2014), Identification, Model Updating, and Validation of a Steel Twin Deck Curved Cable-Stayed Footbridge, Computer-Aided Civil and Infrastructure Engineering, 29, 703–722.

Caesar, B. (1987), Updating system matrices using modal test data, in *5th Int. Modal Analysis Conference*, London, England, 453-459.

Casalegno,C., Ceravolo, R., Chiorino M.A., Pecorelli M.L.& Zanotti Fragonara, L. (2014), Soil-Structure Modeling And Updating of The Regina Monte Regalis Basilica At Vicoforte, Italy, *SAHC2014 – 9th International Conference on Structural Analysis of Historical Constructions* Mexico City, Mexico, 14–17 October.

Ceravolo, R., De Marinis, A., Pecorelli, M. L.& Zanotti Fragonara, L. (2017) Monitoring of masonry historical constructions: 10 years of static monitoring of the world's largest oval dome, *In: Structural Control & Health Monitoring* ,John Wiley & Sons, PP.1988-1999, ISSN: 1545-2255.

Ceravolo, R., Pistone, G., Zanotti Fragonara, L., Massetto S. & Abbiati, G. (2016), Vibration-Based Monitoring and Diagnosis of Cultural Heritage: A Methodological Discussion in Three Examples, *International Journal of Architectural Heritage*, **10** (4), 375-395.

Ceravolo, R., Pistone, G., Zanotti Fragonara, L., Massetto, S., & Abbiati, G. (2014), Vibration-Based Monitoring and Diagnosis of Cultural Heritage: A Methodological Discussion in Three Examples, *International Journal of Architectural Heritage*, 10:4, 375-395, DOI: 10.1080/15583058.2013.850554.

Chen, H.P. & Maung, T.S. (2014),Regularised finite element model updating using measured incomplete modal data, *Journal of Sound and Vibration*,**333**, 5566–5582. http://dx.doi.org/10.1016/j.jsv.2014.05.051.

Chiorino, M.A., Ceravolo, R., Spadafora, A, Zanotti Fragonara, L. & Abbiati, G. (2011), Dynamic Characterization of Complex Masonry Structures: The Sanctuary of Vicoforte. *International Journal of Architectural Heritage*, **5**(3), 296-314. doi: 10.1080/15583050903582516.

Chiorino, M.A., Roccati, R., D'Addato, C., Aoki, T., C. Calderini, Spadafora, A. (2006), Monitoring and modeling strategies for the world's largest elliptical dome at Vicoforte, *Proc. 5th Int. Conf. on Structural Analysis of Historical Constructions* (SAHC), New Delhi, Vol. 2, 1167-1176.

Chiorino, M.A., Spadafora A, Calderini C., & Lagomarsino, S. (2008) Modeling Strategies for the World's Largest Elliptical Dome at Vicoforte, *International Journal of Architectural Heritage*, pp.274-303, ISSN: 1558-3058.

Chow, J.Y.J. (2014), Activity-Based Travel Scenario Analysis with Routing Problem Reoptimization, *Computer-Aided Civil and Infrastructure Engineering*, **29**(2), SN-1467-8667, DOI:10.1111/mice.12023, P-91-106.

Farrar, C.R. & Worden, K. (2007), An introduction to structural health monitoring, *Philosophical Transaction of the Royal Society A: Mathematical Physical and Engineering Science*, **365**, 303–315. http://dx.doi.org/10.1098/rsta.2006.1928.

Friswell, M.I., Mottershead, J.E. & Ahmadian H. (2001) Finite-element model updating using experimental test data: parametrization and regularization, *Philosophical Transaction of the Royal Society A: Mathematical Physical and Engineering Science*, **359,** 169–186. http://dx.doi.org/10.1098/rsta.2000.0719.

Gentile, C., Saisi, A.E., Cabboi, A. (2017) From continuous vibration monitoring to FEM-based damage assessment: Application on a stone-masonry tower. Construction and Building Materials, ISSN: 0950-0618, http://hdl.handle.net/11311/1032375.

Green, A.E. & Lindsay, K.A. (1972), Thermoelasticity, *Journal of Elasticity*, **2**,1-7.

Hoff, C. J., Bernitsas, M. M., Sandstrom, R. E. & Anderson, W. J. (1984), Inverse Perturbation Method for Structural Redesign with Frequency and Mode Shape Constraints, *AIAA Journal*, **22**(9), 1304–1309. http://dx.doi.org/ 10.2514/3.8777.

Humbert, L., Thouverez, F. & Jezequel, L. (1999), Finite element dynamic model updating using modal thermoelastic fields, *Journal of Sound and Vibration*, **228**(2),397-420.

Jiang, X. & Adeli, H. (2008), Neuro-genetic algorithm for non-linear active control of structures. International Journal for Numerical Methods in Engineering, *International Journal for Numerical Methods in Engineering*, **75**(7), PB-John Wiley & Sons, Ltd., SN-1097-0207, DOI:10.1002/nme.2274, P-770-786.

Kanev, S., Weber, F. & Verhaegen, M. (2007), Experimental validation of a finite-element model updating procedure, *Journal of Sound and Vibration*, **300**, 394–413. http://dx.doi.org/10.1016/j.jsv.2006.05.043.

Kazemnia Kakhkia, E., Mahmoud Hosseinib, S. & Tahani, M. (2016) Ananalytical solution for thermoelastic damping in a micro-beam based on generalized theory of thermoelasticity and modified couple stress theory, *Applied Mathematical Modelling*, **40**, 3164–3174. http://dx.doi.org/10.1016/j.apm.2015.10.019.

Kiani, Y. & Eslami, M.R. (2016), The GDQ approach to thermally nonlinear generalized thermoelasticity of a hollow sphere, International Journal of Mechanical Sciences, **118**, 195–204. http://dx.doi.org/10.1016/j.ijmecsci.2016.09.019.

Kiani, Y. & Eslami, M.R. (2017), Nonlinear generalized thermoelasticity of an isotropic layer based on Lord Shulman theory, *Journal of the Mechanics and Physics of Solids*, **61**, 245-253. http\\dx.doi.org/10.1016/j.euromechsol.2016.10.004.

Lee, E.T. & Eun H.-C. (2009), Update of corrected stiffness and mass matrices based on measured dynamic modal data, *Applied Mathemathical Modelling*, **33**, 274–2281. http://dx.doi.org/10.1016/j.apm.2008.06.004.

Lee, E.T., Rahmatalla, S. & Eun, H.-C. (2011a), Estimation of parameter matrices based on measured data, *Applied Mathemathical Modelling*,**35**, 4816–4823 http://dx.doi.org/10.1016/j.apm.2011.03.048.

Lee, E.T., Rahmatalla, S. & Eun, H.-C. (2011b) Integrated mathematical forms for update of physical parameter matrices of damped dynamic system, *Applied Mathemathical Modelling*,1167-1174. http://dx.doi.org/10.1016/j.apm.2011.03.048.

Li, W.M. & Hong, J.Z. (2011), New iterative method for model updating based on model reduction, *Mechanical Systems and Signal Processing*. **25**,180–192. http://dx.doi.org/10.1016/j.ymssp.2010.07.009.

Link, M. (1986), Theory of a method for identifying incomplete system matrices from vibration test data, *Zeitschrift für Flugwissenschaften und Weltraumforschung*, **9**(2), 76-82.

Link, R. J. & Zimmerman, D. (2007), An Approach for Model Updating of a Multiphysics MEMS Micromirror, *Journal of Dynamic Systems, Measurement, and Control*, **129**, 357-366. http://dx.doi.org/10.1115/1.271977.

Lord, H.W. & Shulman, Y. (1967), A Generalized Dynamical Theory of Thermoelasticity, *Journal of the Mechanics and Physics of Solids*, **15**, 299-309.

Merce, R.N., Doz, G.N., Vital de Brito, J.L., Macdonald, J.H.G. and Friswell, M.I. (2007), Finite element model updating of a suspension bridge, In Inverse Problems, Design and Optimization Symposium Miami, Florida, U.S.A., April 16-18, 2007.

Moller, P.W. and Friberg, O., (1998), Updating large finite element models in structural dynamics, AIAA Journal, **36**(10), 1861-1868.

Mottershead, J. & Friswell, M. (1993), Model updating in structural dynamics: a survey, *Journal of Sound and Vibation*, **167**, 347–375. http://dx.doi.org/10.1006/jsvi.1993.1340.

Mottershead, J.E., Link, M., Friswell, M.I. (2011), The sensitivity method in finite element model updating: A tutorial, Mechanical Systems and Signal Processing, 25, 2275–2296.

Nazmul, S., Adeli, H., (2016), Physics-based search and optimization: Inspirations from nature. Expert Systems, Expert Systems. VL-33, IS-6, SN-1468-0394, DOI:10.1111/exsy.12185, P-607-623.

Novello G., Piumatti P. (2012), La Geometria come filo di Arianna: note di approfondimento sul rapporto ideazione-costruzione della più grande cupola di forma ovata del mondo, *Disegnare Con...* Dipartimento di Architettura e Pianificazione Territoriale - Università di Bologna, pp.167-176, ISSN: 1828-5961.

Nowinski, J.L. (1978), Theory of Thermoelasticity with Applications. Sijthoff and Noordhoff, Int. Publ. Alphen Aan Den Rijn.

Parkus, H. (1968), Thermoelasticity, Blaisdell Pub. Co., Waltham Massachussetts.

Pau, A. & Vestroni, F. (2008), Vibration analysis and dynamic characterization of the Colosseum, *Structural Control Health Monitoring*, **15**, 1105-1121.

Pecorelli, M.L., Ceravolo, R., De Lucia, G. & Epicoco, R. (2017) A vibration-based health monitoring program for a large and seismically vulnerable masonry dome. *Journal of Physics. Conference Series*, **842**.

Peeters, Jeroen, et al. (2015), Updating a finite element model to the real experimental setup by thermographic measurements and adaptive regression optimization, *Mechanical Systems and Signal Processing* **64,** 428-440.

Ramos, L.F., Marques, L., Lourenço, P.B., De Roeck, G., Campos-Costa, A. & Roque, J. (2010), Monitoring historical masonry structures with operational modal analysis: two case studies, *Mechanical System and Signal Processing*, **24**, 1291-1305.

Sarma, K. C. & Adeli, H. (2006), Fuzzy Genetic Algorithm for Optimization Of Steel Structures, *Journal of Structural Engineering*, **126**(5), 596-604.

Sarmandi, H., Karamodin, A. & Entezami, A. (2016) A new iterative model updating technique based on least squares minimal residual method using measured modal data, *Applied Math Modelling* ,**40**, 10323-10341. http://dx.doi.org/10.1016/j.apm.2016.07.015.

Siddique, N. and Adeli, H., (2013), Computational Intelligence - Synergies of Fuzzy Logic, Neural Networks and Evolutionary Computing, Wiley, West Sussex, United Kingdom, pp. 512.

Sidhu, J. & Ewins, D. J. (1984), Correlation of finite element and modal testing studies of a practical structure. *In 2nd Int. Modal Analysis Conference*, Orlando, USA, pp. 756-762.

Shan, J., Ouyang, Y., Yuan, H., W. Shi, W. (2016), "Seismic data driven identification of linear physical models for building structures using performance and stabilizing objectives," *Computer-Aided Civil and Infrastructure Engineering*, 31:11, pp. 846-870.

Sun, H. & Betti, R. (2015), A Hybrid Optimization Algorithm with Bayesian Inference for Probabilistic Model Updating, *Computer-Aided Civil and Infrastructure Engineering*, 30, 602–619.

Sun, K., Yonghui Z. & Haiyan H. (2015), Identification of temperature-dependent thermal–structural properties via finite element model updating and selection, *Mechanical Systems and Signal Processing*, **52,** 147-161.

Szekeres, A. (1980), Equation System of Thermoelasticity Using the Modified Law of Thermal Conductivity, Periodica Polytechnica, **24**,253-261.

Villarrubia, G., Juan, F., De Paz, J.F., Chamoso, P., De la Prieta, F. (2018), Artificial neural networks used in optimization problems, *Neurocomputing*, **272**, 10–16.

Yuan, Z., Kaiping Y. & Yunhe B. (2018), A multi-state model updating method for structures in high-temperature environments., *Measurement*, **121**, 317–326.